Synthesis, Structural, Electrical and Dielectical Properties of ZnO Nanoparticles Synthesized by Sonochemical Route

Jazi Abdullah Mohammed Abdulwahed

Physics Department, Umm Al-Qura University College in Qunfudah-Female-KSA

jaabdulwahed@uqu.edu.sa

Abstract

In the present work, simple sonochemical route was used for synthesizing ZnO nanoparticles, by using the ultrasonication time 7 min at room temperature, atmospheric pressure and neutral pH. The structure and morphology of ZnO nanoparticles were investigated by X-ray diffraction (XRD), energy dispersive X-ray analysis (EDX), and transmission electron microscope (TEM). Some structural characteristics of the ZnO nanoparticles as average crystallite size using Scherrer and Williamson Hall methods, lattice strain, and dislocation density were estimated. XRD analysis confirmed a good crystalline structure (hexagonal) of the obtained ZnO nanoparticles. Transmission electron microscopy images of the ZnO nanoparticles reveal that the ZnO nanoparticles in hexagonal morphology with typical diameters of about 38-49 nm. ac and dc electrical properties of the synthesized ZnO nanoparticles were studied. The dependence of temperature of ac and dc conductivity was measured in a temperature range (303- 453 K).

Keywords: Sonochemical route, ZnO Nanoparticles, electrical and dielectical Properties, EDAX, TEM

1- Introduction

ZnO has become an attractive nanomaterial for scientific research, due to its unique properties. ZnO is applicable in UV-light emitters, transparent high-power electronics, sensors, acoustic devices, piezo-electric transducers, ultraviolet photodetectors, and in biomedical systems [1-8]. Many efforts have been made for synthesizing ZnO nanoparticles by using different methods as physical vapor deposition, chemical vapor deposition hydrothermal, solvothermal, sol–gel, chemical precipitation and Sonochemical method [9-14].

Sonochemical technique is interested in conception the effect of ultrasound in formation acoustic cavitation in liquids which creating enhancement of the solution chemical activity [13-16]. The sound wave can therefore not directly increase the internal energy of a molecule. Acoustic cavitation conducts; creation, growth, and implosive collapse of bubbles in the liquid. The bubbles collapse produces a reinforcement of energy inside

the bubble, which resulting in high temperatures and pressures. The elevated temperatures and pressures performed the chemical excitation of the materials that was inside of or in the direct surroundings of the bubbles and increase the chemical activity. Sonochemical is considered a green and practical method and has been confirmed to be an adequate method to prepare new materials [13-16].

Herein, a simple sonochemical route was carried out to synthesis ZnO nanoparticles. The structure, morphology and electrical properties of the obtained ZnO nanoparticles were investigated using several analysis tools. Electrical properties; ac and dc electrical conductivity were studied in a wide range of frequency and temperature.

2- Experimental Procedures

ZnO nanoparticles were synthesized by the following procedure: Zn^{2+} solution had been prepared firstly by dissolving a determined amount of zinc acetate [$Zn(CH_3COO)_2.2H_2O$] in 100 mL NH_3H_2O. Then (1 M) of sodium hydroxide [NaOH] was added to the Zn^{2+} solution. All these processes were carried out at room temperature. After that, deionized water was added till the final concentration became 1 M Zn^{2+} solution. Ultrasonication process was applied on a 25 mL of the obtained solution for 7 min and the temperature during the sonication process was 40°C. The resulting white color product was centrifuged (5 min, 4500 rpm) and washed with distilled water for three times. The obtained white precipitate was dried in air in a laboratory oven at 80 °C for 24 h.

The structure of the synthesized ZnO nanoparticles was characterized by X-ray diffractometer (XRD, Philips, X'pert, Cu Ka), transmission electron microscopes (TEM, JEOL, 2010). Compacted discs of the synthesized ZnO nanoparticles were prepared to study the dielectric and electrical parameters. The compressed discs were prepared by applying constant pressure (5 t) at the same amounts of the used nanomaterials (about 0.3 g), to obtain a constant thickness of the discs. The capacitance, C, impedance, Z and loss tangent, tanδ were measured directly by a computer controlled HIOKI 3532-50 LCR meter in the frequency range 42 Hz to 5 MHz. A KEITHLEY 6517A electrometer connected directly to the sample was used to measure the dc electrical conductivity of the sample. For dc and ac measurements a particular designed holder was utilized. By using temperature controller, the temperature of the system was adjusted in a specified range (303–453 K) with accuracy about ±1 K.

3. Results and Discussion

3.1 Structure and Morphology

Figure 1 shows a typical XRD spectrum of ZnO nanoparticles synthesized by sonochemical method. The XRD spectra indicate that the ZnO crystal has a hexagonal structure, and its lattice constants are (a = b = 0.3251 nm) and (c = 0.5212 nm) as in standard JCPDS data. XRD pattern declares that ZnO nanoparticles were free of contaminations because, the pattern does not contain any XRD peaks other than ZnO peaks. From Fig.1, the observed sharp and intense peaks at XRD pattern confirm that the prepared ZnO nanoparticles are of high crystalline nature with hexagonal phase.

The crystallite size, D, has been determined using the formula of Debye–Scherrer [3] as follows:

$$D = 0.9\,\lambda / \beta \cos\theta \qquad (1)$$

Where, λ is the wave length of the used X-ray (1.54060 Å), β is the angular peak width at half maximum in radians and θ is Bragg's diffraction angle. From the XRD pattern, the synthesized ZnO nanoparticles are listed as wurtzite hexagonal closely packed structure and the lattice constants a and c were calculated by using the interplanar distance d and (hkl) values of the XRD profile from the following equation [17],

$$1/d^2 = 4/3\left[\frac{h^2 + hk + l^2}{a^2}\right] + l^2/c^2 \qquad (2)$$

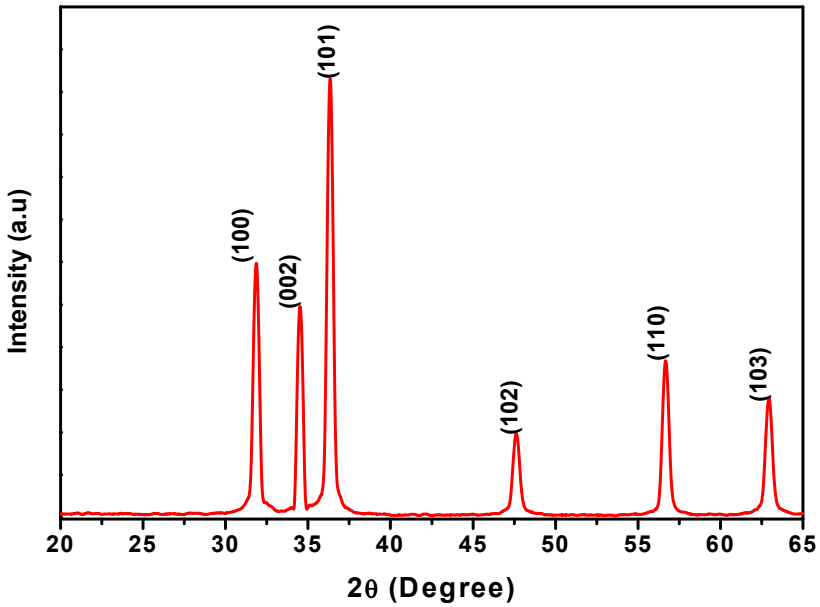

Fig. 1 XRD pattern of the obtained ZnO nanoparticles

Table 1 shows the determined lattice parameters, which are corresponded to those presented in standard JCPDS data. The crystallite size and the lattice strain, using

Williamson-Hall (WH) method (Eq. 3) were estimated by inspection the diffraction peaks shape. The procedure of WH calculations was achieved for every peak of the obtained ZnO nanoparticle. The crystallite size, **D**, and the strain, **ε**, are related to the full width at half maximum (FWHM), **β**, by the following equation:

$$\beta^* = d^* \varepsilon + 1/D \qquad (3)$$

Where $\beta^* = \beta \cos\theta / \lambda$ and $d^* = 4 \sin\theta / \lambda$; θ is the Bragg angle and **λ** is the used wavelength. From plotting **β cos θ** against **4 sinθ,** the intercept of the plot gives **1/D** and the slope gives the strain as shown in Fig. 2 [17-18]. Table 1 shows crystallite size values for the prepared samples estimated by Scherer and Williamson-Hall methods.

The defects and vacancies amount in the crystal (dislocation density), **S**, can be calculated by using the crystallite size (D), from the following equation [12,17]:

$$S = 1/D^2 \qquad (4)$$

Table 1 The characteristics of the ZnO nanoparticles synthesized values

NO.	2θ (101), (°)	FWHM, (rad), (10^{-2})	D (nm)		d, (nm)	a (nm)	C, (nm)	S (10^{-3})	ε, (10^{-3})
			Scherer	WH					
S_1	36.3327	0.2184	38.42	48.59	0.2476	0.3248	0.5205	0.6776	0.9055

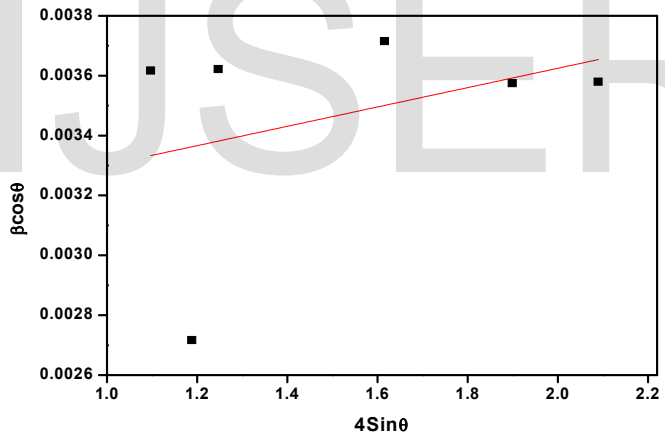

Fig. 2 plotting of βcosθ against 4εsinθ using W-H method

To check the purity level of the synthesized ZnO nanoparticles, EDX analyses was carried out. Figure 3 shows the EDX spectrum of ZnO nanoparticles synthesized by sonochemical method. The strong peaks showed in the spectrum referred to Zinc and oxygen elements, which indicates that the synthesized nanoparticles have Zn and O elements only.

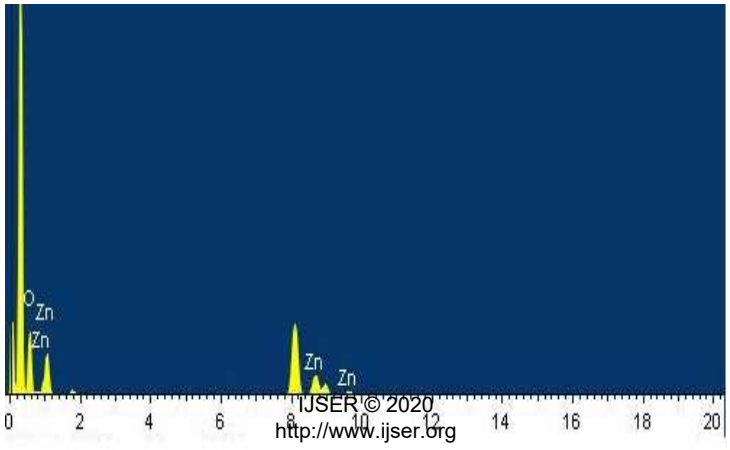

Fig.3 EDX spectrum of ZnO nanoparticles.

TEM analysis was carried out to investigate the shape and the size of the synthesized ZnO nanoparticles (30-50 nm). Figure 4 displays the TEM image of the prepared ZnO nanoparticles. ZnO nanoparticles are observed that they have a spherical-like and rod shapes. All the ZnO nanoparticles approximately appeared as clusters of nanorods shape due to the coalescing of the small nanoparticles and forming larger particles.

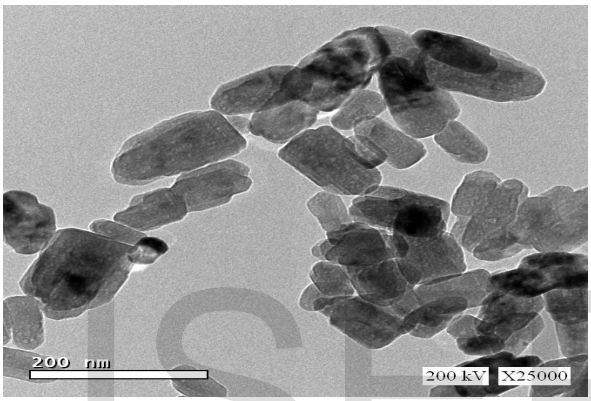

Fig.4 HRTEM image of the synthesized ZnO nanoparticles

3.2 Electrical Properties of ZnO nanoparticles

The dc electrical conductivity of ZnO nanoparticles has temperature dependence as shown in Fig. 5. It is obvious that the σ_{dc} conductivity increases with increasing the temperature. According to the following equation:

$$\sigma_{dc} = \sigma_{o1} \exp\left(-\frac{\Delta E_{\sigma 1}}{kT}\right) + \sigma_{o2} \exp\left(-\frac{\Delta E_{\sigma 2}}{kT}\right) \quad \textbf{(5)}$$

In the above equation σ_{o1} and σ_{o2} represents the pre-exponential factor for regions 1 and 2, also, $\Delta E\sigma_1$ and $\Delta E\sigma_2$ are the dc conduction activation energy for the mentioned two regions respectively, while k is the Boltzmann's constant. Values of $\Delta E\sigma_1$ and $\Delta E\sigma_2$ can be estimated from the slopes of the obtained straight lines which showing that there are two conduction mechanisms in the studied range of temperature (303- 453 K). The resulted values of $\Delta E_{\sigma 1}$ and σ_{o1} for region (1) are reported as, 0.069 eV, 0.044 $(\Omega m)^{-1}$ at the lower temperature range, respectively and the values of $\Delta E_{\sigma 2}$ and σ_{o2} for region (2) are 0.207 eV and 3.706 $(\Omega m)^{-1}$ at the higher temperature range, respectively. It is

expected in intrinsic semiconductors that; the activation energy should be less than half of the optical energy gap and this is matching with the obtained values of $\Delta E_{\sigma 1}$ and $\Delta E_{\sigma 2}$ for ZnO nanoparticles [19]. The activation energy values in low and high temperature ranges are in good agreement with previous reported works of ZnO nanoparticles [20,21]. The results of the electrical conductivity declare that the mechanism of electrical conduction is thermally activated process. Also, the dc conductivity increases exponentially in the applied temperature range (303- 453 K).

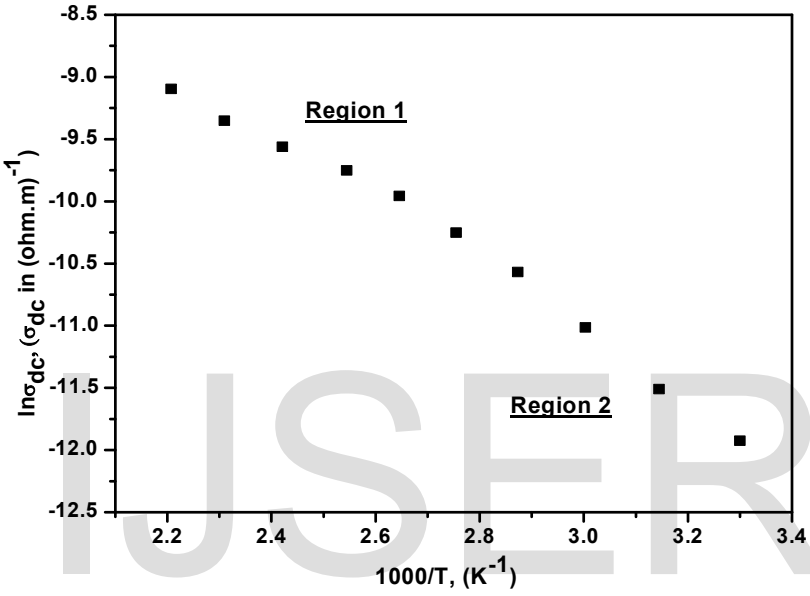

Fig.5. The dc electrical conductivity (σ_{dc}) against temperature for ZnO nanoparticles.

Figure 6 displays the calculated electrical conductivity $\sigma_{ac}(\omega)$ for ZnO nanoparticles at different values of frequency (200 kHz-5 MHz) and temperature (303- 453 K) which can be calculated from the following equation, in which ω is the angular frequency (2πf), [22, 23]:

$$\sigma_{tot.ac}(\omega) = \sigma_{ac}(\omega) + \sigma_{dc}(\omega \to 0) \quad \textbf{(6)}$$

Figure 6 indicates that the ac electrical conductivity curve of ZnO nanoparticles is a frequency dependent while the dc electrical conductivity is increased with increasing temperature (temperature dependent) as shown in fig.5. The ac conductivity decreases with increasing the frequency and at higher frequency values, the ac conductivity displays weakly temperature dependence. Also, the relation of $\sigma_{ac}(\omega) = f(1/T)$ has a linear behavior at different activation energies (at different regions), the first with weak

temperature dependence and the other with strong temperature dependence. This mechanism is attributed to the hopping between states near the mobility edges where the density of states is considered constant [22-24].

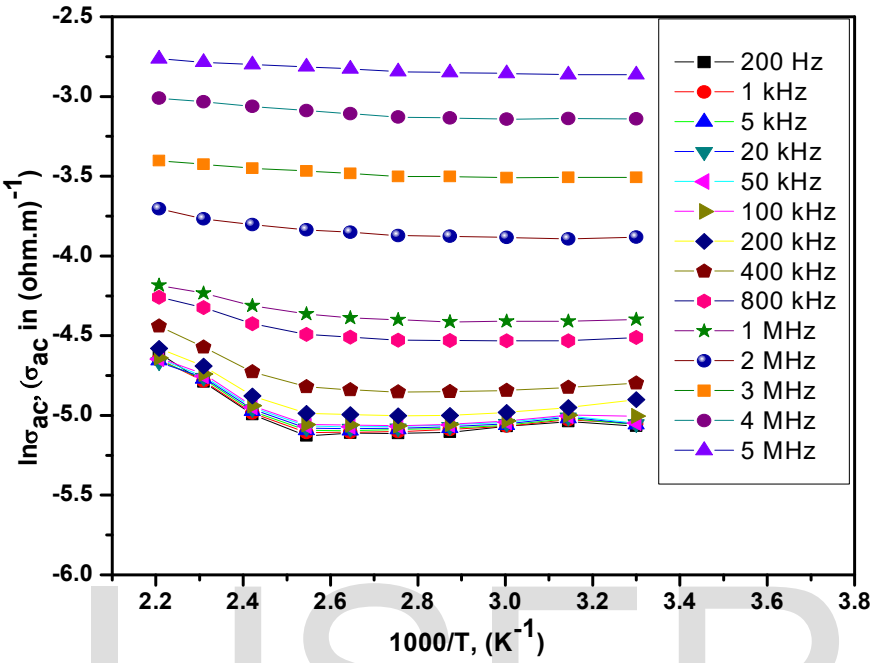

Fig.6 Frequency dependence of $\sigma_{ac}(\omega)$ for ZnO nanoparticles at different frequencies and temperatures

According to Arrhenius equation, the activation energy of the $\Delta E(\omega)$ is calculated at different frequencies from the slope of lines in figure 6 in the higher temperature range, which shows that the temperature dependence of ac conductivity is a thermally activated process:

$$\sigma_{ac}(\omega) = \sigma_o \exp\left(\frac{-\Delta E(\omega)}{kT}\right) \quad (7)$$

where σ_o is constant, $\Delta E(\omega)$ is the ac electrical activation energy and T is the absolute temperature. Figure 7 shows the frequency dependence of the ac activation energy $\Delta E(\omega)$ for ZnO nanoparticles. The values of $\Delta E(\omega)$ is nearly constant at the lower frequencies and then decreased with the increasing of the applied frequency. This action is due to the contribution of the applied frequency with the conduction mechanism, which ensures that the hopping conduction is the predominant mechanism. The increase of the frequency promotes the electronic jumps between the localized states and decreases the activation energy $\Delta E(\omega)$. The resulted activation energy is low and

changes a slightly with frequency. The lower value of activation energy denotes that the electric conduction carried out by charge carriers hopping between the defect states close to the Fermi level. By comparison between the bulk ZnO and nanocrystals a difference in their values was noticed, the obtained values of the ac activation energy (0.02–0.13 eV) are lower than the values of the bulk ZnO (0.35–0.63), which enhance the electrical properties of semiconductor materials, that confirms the unique properties of the nanomaterials [25].

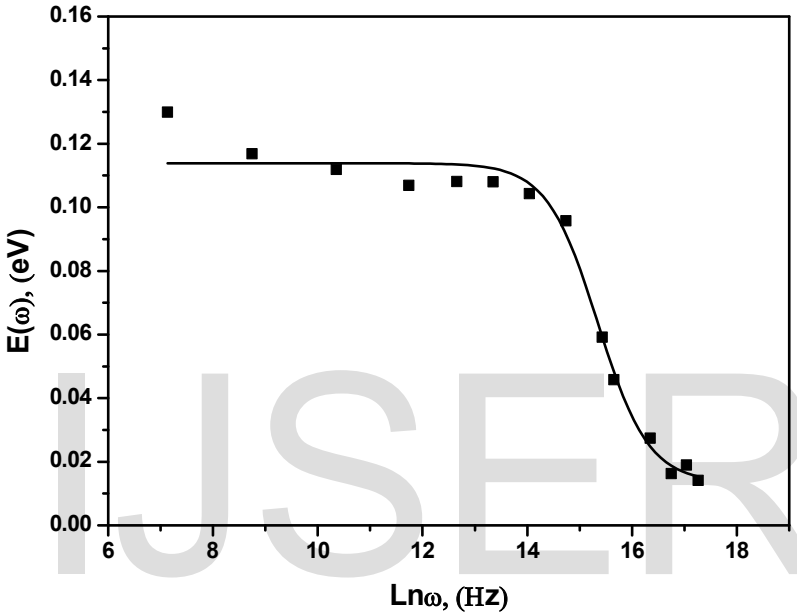

Fig.7 ac activation energy ΔE(ω) frequency dependence for ZnO nanoparticles

The relation between $\ln\sigma_{ac}$ (ω) and ln(ω) for ZnO nanoparticles at the temperature range (303–453 K) is displayed in figure 8, from which it can be noticed that the ac conductivity increases nearly linearly with frequency. The ac conductivity can be estimated from the following equation [25]:

$$\sigma_{ac}(\omega) = A\omega^{s} \quad (8)$$

where s is the frequency exponent and A is the constant dependent on temperature. The frequency exponent depends on the material temperature T and varies from 0 to 1; for ideal Debye type samples it is equal to 1. The exponent s related to the charge carriers or extrinsic dipoles which arises from the defects or impurities presence. The frequency exponent s values were calculated from the slopes of linear part of the relation of ln

$\sigma_{ac}(\omega) = f(\omega)$ at the higher frequency range, at different temperature range (303-453 K) for ZnO nanoparticles.

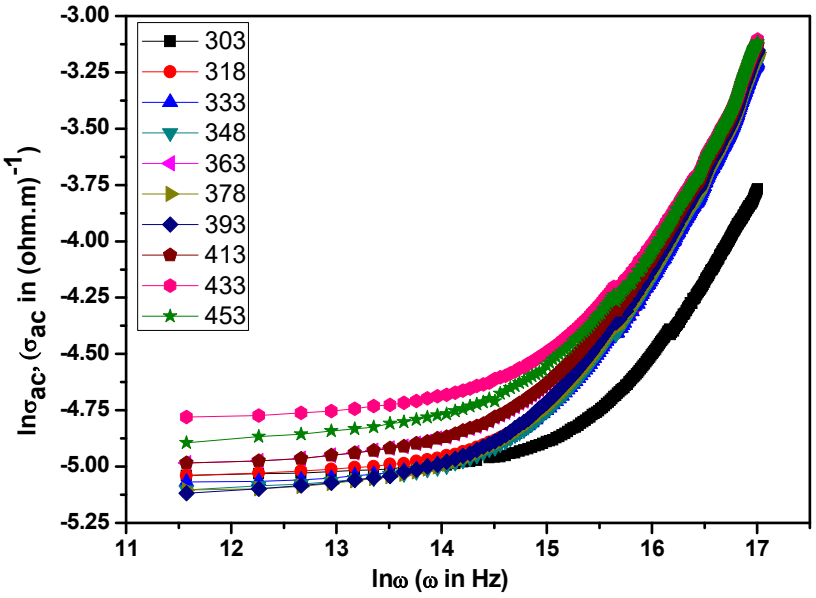

Fig.8 The relation between $\ln\sigma_{ac}$ (ω) and ln(ω) for ZnO nanoparticles at the temperature

The temperature dependence of s for ZnO nanoparticles is shown in Fig. 9. It is clear from this figure that s decreases and 1-s increases as the temperature increases for the prepared sample. The values of exponent s and (1-s) of ZnO nanoparticles are estimated from the slope.

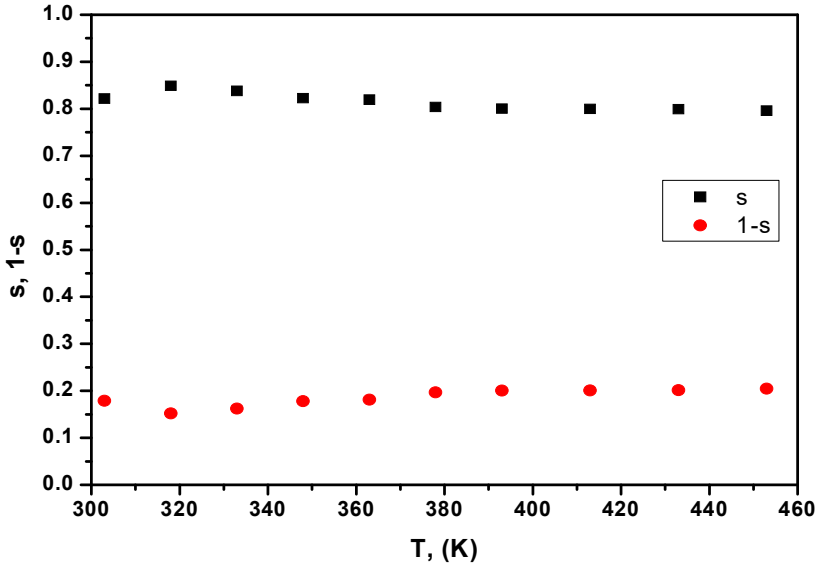

Fig. 9 The temperature dependence of s for ZnO nanoparticles

Various theories tried to interpret the conduction mechanism of $\sigma_{ac}(\omega)$ with temperature as; quantum-mechanical tunneling model (QMT), large polaron tunneling model (LPT), small polaron tunneling model (SPT) and correlated barrier-hopping model (CBH). The ac conduction theoretical explanations were applied on the nanomaterials to clarify the dependence of $\sigma_{ac}(\omega)$ and s, on frequency and temperature. The values of the exponent s are around 0.8 or equal 0.8 with different times, and increase slightly with increasing temperature. So, for the present data the quantum-mechanical tunneling (QMT) model can be considered the suitable model for explaining the frequency dependence of $\sigma_{ac}(\omega)$.

3.3 Dielectical Properties of ZnO nanoparticles

The dielectric constant (ε_1) and dielectric loss (ε_2) were calculated by using the measured parameters according to the following relations [24, 26, 27].

$$\varepsilon_1 = \frac{Ct}{\varepsilon_0 A} \quad \textbf{(9)}$$

$$\varepsilon_2 = tan\delta * \varepsilon_1 \quad \textbf{(10)}$$

where, t is the thickness and A is the area of the prepared pallets, ε_o is the free space permittivity. Figures 10,11 displays the frequency dependence of ε_1 and ε_2 of ZnO nanoparticles at different temperatures range (303-453 K) respectively. It is obvious that ε_1 and ε_2 are frequency dependent at higher temperature while their frequency becomes weaker with decreasing temperature. The decrease in ε_1 and ε_2 with frequency can be attributed to dielectric polarization [28-31].

The low frequencies lead to contribution of the polarizability between components, orientational and interfacial relaxational and electronic deformational. Along the direction of the field, the dipoles are stratified themselves for achieving completely contribution to the polarization. Because orientational polarization takes time longer than the ionic and electronic polarization, it increases with the frequency decreasing [32].

The dielectric constant (ε_1) increases with temperature due to the orientational polarization which is linked to the thermal motion of the molecules. Also, at high temperature dielectric constant (ε_1) increases with increasing the value of orientational polarization which carried out by simplifying the orientation of dipoles [33,34]. The values of dielectric constant (ε_1) and dielectric loss (ε_2) increase with increasing temperature for all frequencies [33,34].

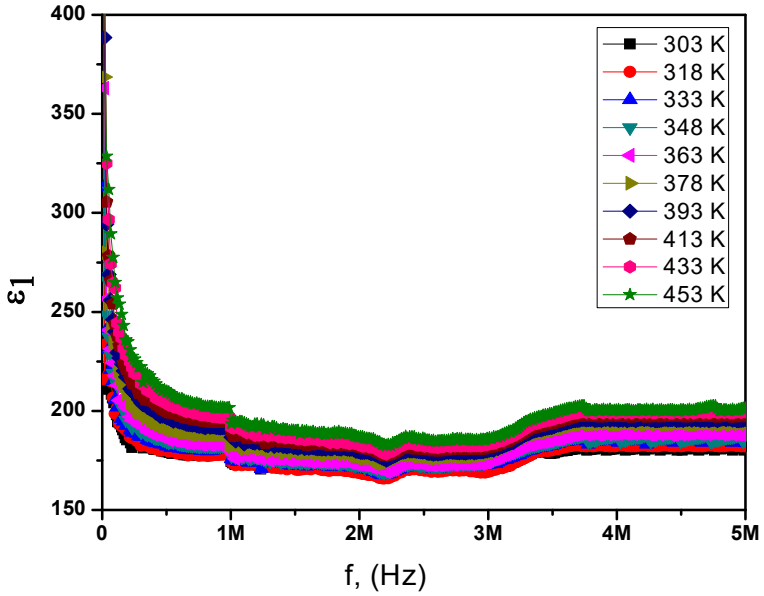

Fig.10 Frequency dependence of ε_1 of ZnO nanoparticles at different temperatures

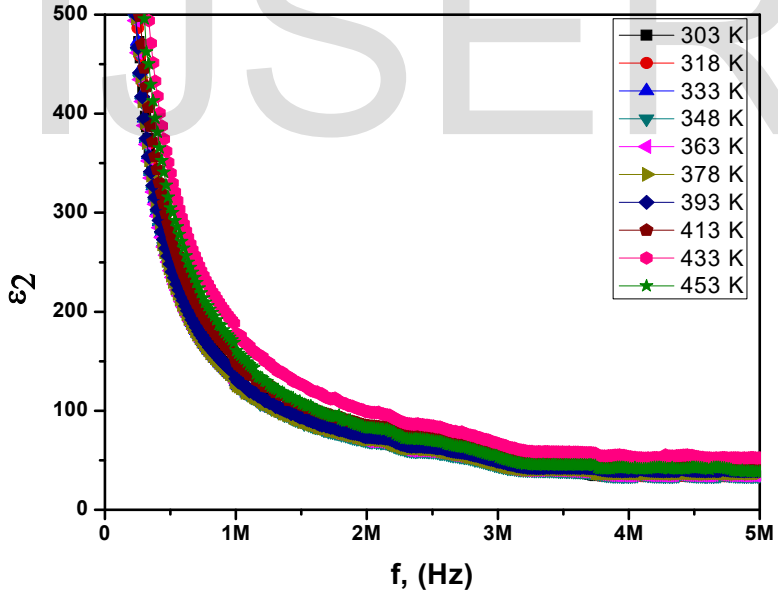

Fig. 11 Frequency dependence of ε_2 of ZnO nanoparticles at different temperatures

Figure 12 shows the dielectric loss tangent (tan δ) variation with frequency at different temperatures (303-453 K), from which it is clear that tan δ decreases with frequency. Higher values of dielectric loss appear at lower frequencies. The decrease of dielectric loss is achieved when the jumping rate of the charge carriers delays at the field [35].

Dialectical loss (ε_2) and dielectric loss tangent are generally decrease with the increase of frequency. Koop's model adopts the investigation that tangent loss has high values at lower frequencies. Koop's model illustrates that at lower frequencies the resistivity is high and the effect is of the grain boundaries.

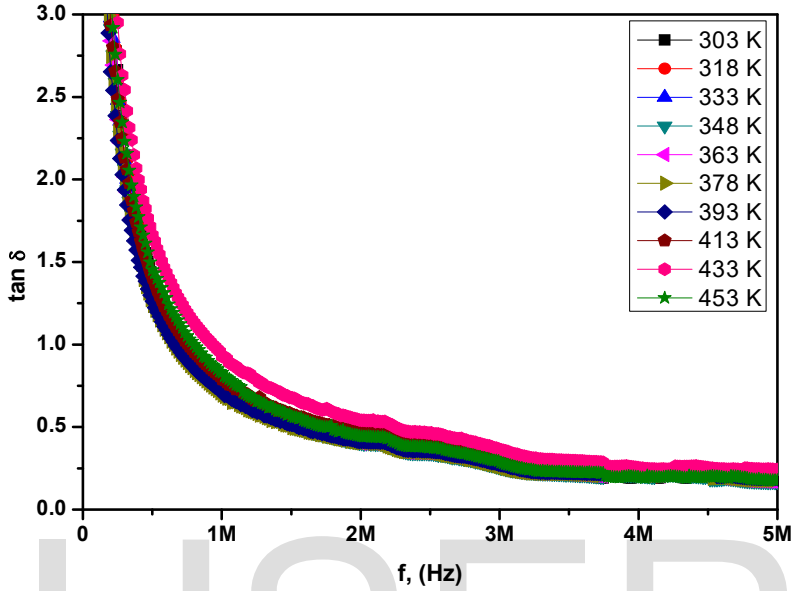

Fig. 12 Dielectric loss tangent (tan δ) variation with frequency at different temperatures

4. Conclusion

In this work, synthesis of a hexagonal structure ZnO nanoparticles were successfully achieved using Ultrasonication process**.** XRD studies emphasized the hexagonal structure of the synthesized nanoparticles and the crystallite size was estimated by both Scherrer and Williamson Hall treatments (average size was 38-49 nm). The image of TEM analysis showed the crystalline and nearly the hexagonal particles with average size that matched with XRD calculations. From the electrical conductivity results it is clear that the mechanism of electrical conduction is thermally activated process. The ac electrical conductivity curve of ZnO nanoparticles is a frequency dependent while the dc electrical conductivity is temperature dependent in the range (303-453 K). This behaviour is attributed to the hopping between states near the mobility edges where the density of states is considered constant. The resulted activation energy is low and changes a slightly with frequency. The values of dielectric constant (ε_1) and dielectric loss (ε_2) increase with increasing temperature for all frequencies. dielectric constant (ε_1) increases with temperature due to the orientational polarization which is linked to the

thermal motion of the molecules. According to the obtained results the synthesized ZnO nanoparticles can be considered as a promising material for semiconductor devices.

References

1. A. Benazir, K. Gomathi, S. Aram, Structural and optical properties of Zn1–xNixO nanoparticles synthesized by co-precipitation method. J. Environ. Nanotechnol. 6, 39–43 (2017)
2. K.P. Kamal, G. Dambaru, A. Venugopal, V.M.A. Mohan, P. Ganngam, L.P. Narasimham, K.S. Hrushi, B.P. Brahma, Green synthesized zinc oxide (ZnO) nanoparticles induce oxidative stress and DNA damage in *Lathyrus sativus* L. Root Bioassay Syst. Antioxid. 6, 35–51 (2017).
3. A.M.O. Dalia, A.M. Mustafa, Synthesis and characterization of zinc oxide nanoparticles using zinc acetate dihydrate and soium hydroxide. J. Nanosci. Nanoeng. 1, 248–251 (2015)
4. S. Sabita, C.B. Subash, P.S. Shankar, P.J. Leela, Synthesis and study of zinc oxide nanoparticles for dye sensitized solar cell. Res. J. Phys. Sci. 5, 6–10 (2017)
5. R.A. Zargar, M. Arora, Synthesis and characterization of ZnO nanoparticles for biomedical applications. Glob. J. Nanomed. 2, 1–3 (2017)
6. K. Zheng, K. Zidek, M. Abdellah, P. Chabera, M.S. Abd El-sadek, T. Pullerits, Effect of metal oxide morphology on electron injection from CdSe quantum dots to ZnO. Appl. Phys. Lett. 102, 163119-1–163119-5 (2013)
7. M. Vaseem, A. Umar, Y.B. Hanh, ZnO nanoparticles: growth, properties, and applications. in *Metal Oxide Nanostructures and their Applications*, ed. by A. Ummer, Y.B. Hanh (5 American Scientific Publishers, Los Angeles, 2010) 1–36.
8. Y. Xie, Y. He, P.L. Irwin, T. Jin, X. Shi, Antibacterial activity and mechanism of action of zinc oxide nanoparticles against *Campylobacter jejuni*. Appl. Environ. Microbiol. 77, 2325–2331 (2001)
9. Z. An-Qi, Z. Lu, S. Li, Q. Dong-Jin, C. Meng, Morphology-controllable synthesis of ZnO nano-microstructures by a solvothermal process in ethanol solution Cryst. Res. Technol. 48, 947–955 (2013)
10. 14. E.R. Shaaban, A.M.A. Mostafa, H. Shokry Hassan, M.S. Abd El-Sadek, G.Y. Mohamed, I. Sharaf, Effect of γ-irradiation on structural and optical ellipsometry parameters of ZnO nanocrystalline. Int. J. Thin Film Sci. Technol. 3, 129–141 (2014)
11. 15. S.D. Lee, S.H. Nam, M.H. Kim, J.H. Boo, Synthesis and photocatalytic property of ZnO nanoparticles prepared by spray-pyrolysis method. Phys. Proc. 32, 320–326 (2012)
12. H. S. Wasly, M. S. Abd El‑Sadek, Mohamed Henini Influence of reaction time and synthesis temperature on the physical properties of ZnO nanoparticles synthesized by the hydrothermal method. Applied Physics A (2018) 124:76, doi.org/10.1007/s00339-017-1482-4
13. Zak, A. Khorsand, H. Z. Wang, Ramin Yousefi, A. Moradi Golsheikh, and Z. F. Ren. "Sonochemical synthesis of hierarchical ZnO nanostructures." *Ultrasonics sonochemistry* 20, no. 1 (2013): 395-400.
14. Luévano-Hipólito, E., and L. M. Torres-Martínez. "Sonochemical synthesis of ZnO nanoparticles and its use as photocatalyst in H 2 generation." *Materials Science and Engineering: B* 226 (2017): 223-233.
15. Kandjani, A. Esmaielzadeh, M. Farzalipour Tabriz, and B. Pourabbas. "Sonochemical synthesis of ZnO nanoparticles: The effect of temperature and sonication power." *Materials Research Bulletin* 43, no. 3 (2008): 645-654.
16. Yadav, Raghvendra S., Priya Mishra, and Avinash C. Pandey. "Growth mechanism and optical property of ZnO nanoparticles synthesized by sonochemical method." *Ultrasonics sonochemistry*15, no. 5 (2008): 863-868.
17. C.M. Jay, M. Sathya, K. Pushpanathan, Effect of pH on crystal size and photoluminescence property of ZnO nanoparticles prepared by chemical precipitation method. Acta Metall. Sin. (Engl. Lett.) 28, 394–404 (2015).

18. K.G. Williamson, H.W. Hall, X-ray broadening from field aluminium and wolfram. Acta Metall. 1, 1–22 (1953).
19. H. S. Wasly, M. S. Abd El‑Sadek, Mohamed Henini Influence of reaction time and synthesis temperature on the physical properties of ZnO nanoparticles synthesized by the hydrothermal method. Applied Physics A, (2018), 124:76.
20. Swaroop, K., C. S. Naveen, H. S. Jayanna, and H. M. Somashekarappa. "Effect of gamma irradiation on DC electrical conductivity of ZnO nanoparticles." In AIP Conference Proceedings, vol. 1665, no. 1. 2015.
21. Mandal, Sanjay Kumar, Puja Dey, and Tapan Kumar Nath. "AC and DC electrical transport studies of (Fe, Co) codoped ZnO nanoparticles." Journal of Vacuum Science & Technology B, Nanotechnology and Microelectronics: Materials, Processing, Measurement, and Phenomena 32, no. 4 (2014): 041803.
22. Hamood, R., MS Abd El-sadek, and A. Gadalla. "Facile synthesis, structural, electrical and dielectric properties of CdSe/CdS core-shell quantum dots." Vacuum 157 (2018): 291-298.
23. El-sadek, MS Abd, I. S. Yahia, and A. M. Salem. "Electronic transport mechanism of CdTe nanocrystalline." Materials Chemistry and Physics 130, no. 1-2 (2011): 591-597.
24. Shkir, Mohd, Mona Kilany, and I. S. Yahia. "Facile microwave-assisted synthesis of tungsten-doped hydroxyapatite nanorods: a systematic structural, morphological, dielectric, radiation and microbial activity studies." Ceramics International 43, no. 17 (2017): 14923-14931.
25. Shinde, M. S., P. B. Ahirrao, and R. S. Patil. "Structural, optical and electrical properties of nanocrystalline ZnS thin films deposited by novel chemical route." Archives of Applied Science Research 3, no. 2 (2011): 311-317.
26. Niu, Haijun, Liwei Zhang, Mingyuan Gao, and Yongming Chen. "Amphiphilic ABC triblock copolymer-assisted synthesis of core/shell structured CdTe nanowires." Langmuir 21, no. 9 (2005): 4205-4210.
27. Yakuphanoglu, F., I. S. Yahia, G. Barim, and B. Filiz Senkal. "Double-walled carbon nanotube/polymer nanocomposites: electrical properties under dc and ac fields." *Synthetic Metals* 160, no. 15-16 (2010): 1718-1726.
28. I.S. Yahia, N.A. Hegab, A.M. Shakra, A.M. AL-Ribaty, Conduction mechanism and the dielectric relaxation process of a-Se75Te25−xGax (x=0, 5, 10 and 15 at wt%) chalcogenide glasses, Physica B 407 (13) (2012) 2476–2485.
29. Sharma, A., and N. Mehta. "Analysis of dielectric relaxation in glassy Se and Se 98 M 2 (M= Ag, Cd and Sn) alloys: A study of metal-induced effects." *The European Physical Journal-Applied Physics*59, no. 1 (2012).
30. Ansari, Sajid Ali, Ambreen Nisar, Bushara Fatma, Wasi Khan, M. Chaman, Ameer Azam, and A. H. Naqvi. "Temperature dependence anomalous dielectric relaxation in Co doped ZnO nanoparticles." *Materials Research Bulletin* 47, no. 12 (2012): 4161-4168.
31. Zamiri, Reza, B. K. Singh, Dibakar Dutta, Avito Reblo, and J. M. F. Ferreira. "Electrical properties of Ag-doped ZnO nano-plates synthesized via wet chemical precipitation method." *Ceramics International* 40, no. 3 (2014): 4471-4477.
32. B. Tareev, Physics of Dielectric Materials, Moscow: Publish-ers, South Pasadena, CA, 1975, U.S.A 187.
33. El-Nahass, M. M., A. A. Atta, E. F. M. El-Zaidia, A. A. M. Farag, and A. H. Ammar. "Electrical conductivity and dielectric measurements of CoMTPP." *Materials Chemistry and Physics* 143, no. 2 (2014): 490-494.
34. Elliott, S. R. "A theory of ac conduction in chalcogenide glasses." *Philosophical Magazine*36, no. 6 (1977): 1291-1304.
35. Koops, C. G. "On the dispersion of resistivity and dielectric constant of some semiconductors at audiofrequencies." *Physical Review* 83, no. 1 (1951): 121.